

## Spin Drag of a Fermi Gas in a Harmonic Trap

O. Goulko,<sup>1</sup> F. Chevy,<sup>2</sup> and C. Lobo<sup>3</sup>

<sup>1</sup>*Physics Department, Arnold Sommerfeld Center for Theoretical Physics, and Center for NanoScience, Ludwig-Maximilians-Universität, Theresienstraße 37, 80333 Munich, Germany*

<sup>2</sup>*Laboratoire Kastler Brossel, CNRS, UPMC, École Normale Supérieure, 24 rue Lhomond, 75231 Paris, France*

<sup>3</sup>*School of Mathematics, University of Southampton, Highfield, Southampton SO17 1BJ, United Kingdom*  
(Received 23 July 2013; published 4 November 2013)

Using a Boltzmann equation approach, we analyze how the spin drag of a trapped interacting fermionic mixture is influenced by the nonhomogeneity of the system in a classical regime where the temperature is much larger than the Fermi temperature. We show that for very elongated geometries, the spin damping rate can be related to the spin conductance of an infinitely long cylinder. We characterize analytically the spin conductance both in the hydrodynamic and collisionless limits and discuss the influence of the velocity profile. Our results are in good agreement with recent experiments and provide a quantitative benchmark for further studies of spin drag in ultracold gases.

DOI: [10.1103/PhysRevLett.111.190402](https://doi.org/10.1103/PhysRevLett.111.190402)

PACS numbers: 03.75.Ss, 05.30.Fk, 34.50.-s, 67.10.-j

In recent years, ultracold atoms have become a unique testing ground for quantum many-body physics. Their study has favored the emergence of novel experimental and theoretical techniques which have led to an accurate quantitative understanding of the thermodynamic properties of strongly correlated dilute gases at equilibrium [1]. An important effort is now devoted to the exploration of the out-of-equilibrium behavior of these systems, and in particular, to the determination of their transport properties. For instance, recent experiments have probed the transport of an ultracold sample through a mesoscopic channel [2], and time of flight expansions have been used to measure the gas viscosity in the strongly correlated regime [3] where it is predicted to be close to the universal limit conjectured by string theory [4].

In this Letter, we focus on spin transport properties of a Fermi gas which have now received considerable attention in the cold atom community [5–11] after previously being studied in the context of liquid <sup>3</sup>He [12], ferromagnetic metals [13], and spintronic materials [14]. Recent measurements of the spin-drag (SD) coefficient [15,16] have shown that the most challenging aspect of these studies is how to extract the homogeneous gas properties from measurements performed in harmonic traps. The trapping potential creates a density inhomogeneity which can significantly alter the transport behavior of the gas because the local mean-free path can vary strongly from point to point in the trap, leading to a coexistence of regions, from hydrodynamic near the cloud center to collisionless at the edge [17]. For the same reason, the velocity during the relaxation to equilibrium is not constant as a function of radius and it is essential that it be accurately known in order to find the correct values of transport coefficients. Previous theoretical attempts to cope with these problems have included making unverified assumptions about the velocity profile of the gas [18–20] or treating the problem

in the hydrodynamic approximation with spatially varying spin diffusivity [17]. In this last work, no quantitative conclusion could be obtained due to the importance of the collisionless regions of the cloud.

Here, we present a systematic study of the spin transport in an elongated harmonic trap based on the Boltzmann equation using a combination of analytical and numerical methods in the dilute limit and for small phase-space density. In this regime, we are able to analyze the behavior of the trapped gas, allowing us to deal *ab initio* with the spatial density changes without any uncontrolled approximations. In particular, we are able to make definite predictions for the spin-drag coefficient and the transverse velocity profile in both the collisionless and hydrodynamic regimes.

Consider an ensemble of spin-1/2 fermions of mass  $m$  confined in a very elongated harmonic trap with axial frequency  $\omega_z$  and transverse frequency  $\omega_x = \omega_y \equiv \omega_\perp \gg \omega_z$ . Each atom has  $s = \pm$  spin with equal numbers of atoms in each spin state. In the initial thermal equilibrium state, the two spin species are separated from each other by an average distance of  $\pm z_0$  along the symmetry axis of the trap, as in Ref. [15]. Then, we let the system relax towards equilibrium and, as observed experimentally, the relaxation of the motion of the centers of mass of the two clouds occurs at a rate  $\propto \omega_z^2/\gamma_{\text{coll}}$ , where  $\gamma_{\text{coll}}$  is the collision rate [15]. In the very elongated limit  $\omega_z \ll \omega_\perp$ ,  $\gamma_{\text{coll}}$ , the momentum and the spatial transverse degrees of freedom are therefore always thermalized, and we can assume that the phase-space density of the spin species  $s = \pm$  is given by the ansatz

$$f_s(\mathbf{r}, \mathbf{p}, t) = f_0(\mathbf{r}, \mathbf{p})[1 + s\alpha(z, t)], \quad (1)$$

where  $f_0$  is the equilibrium phase-space density. As long as interparticle correlations are weak, the single particle phase-space density encapsulates all the statistical

information on the system. In the following, we restrict ourselves to this regime. Since the experiment [15] was performed at unitarity, this condition is achieved when the temperature is much larger than the Fermi temperature  $T_F$ . As a consequence, we can also neglect Pauli blocking during collisions.

Let  $\bar{n}_s(z, t) = \int d^2\mathbf{p} d^3\mathbf{p} f_s(\mathbf{r}, \mathbf{p}, t) = \bar{n}_0(z)[1 + s\alpha(z, t)]$  be the 1D density along the axis of the trap, where  $\mathbf{p} = (x, y)$ . Integrating Boltzmann's equation over  $x$  and  $y$ , we have

$$\partial_t \bar{n}_s + \partial_z \Phi_s = 0, \quad (2)$$

where  $\Phi_s = \int d^2\mathbf{p} d^3\mathbf{p} f_s(\mathbf{r}, \mathbf{p}) v_z$  (with  $v_z = p_z/m$  the axial velocity) is the particle flux of spin  $s$  in the  $z$  direction. If the trap is very elongated, we can define a length scale  $\ell$  much smaller than the axial size of the cloud but much larger than its transverse radius, the interparticle distance, or the collisional mean-free path, so that for distances smaller than  $\ell$  along the  $z$  axis, the physics can be viewed as being equivalent to that of an infinitely elongated trap ( $\omega_z = 0$ ) with the same central density. In this setup, the two spin species are pulled apart by a force  $\mathbf{F}_s = -\nabla V - (\nabla P_s)/n_s$ , where  $V$  is the spin-independent trapping potential,  $P_s$  is the pressure of the spin species  $s$ , and  $n_s(\mathbf{r}, t) = \int d^3\mathbf{p} f_s(\mathbf{r}, \mathbf{p}, t)$  is the associated density. We consider here a classical ideal gas, for which  $P_s = n_s k_B T$ . Using the ansatz (1), we see that the force field is uniform and is given by  $\mathbf{F}_s = -s k_B T \partial_z \alpha \mathbf{e}_z \equiv F_s \mathbf{e}_z$ , where  $\mathbf{e}_z$  is the unit vector along  $z$ , since  $\partial_z \alpha$  can be considered constant to leading order on the length scale  $\ell$ .

In the regime of linear response, the particle flux is proportional to the drag force and we can write  $\Phi_s = G F_s$ , where  $G$  is the ‘‘spin conductance’’ that *a priori* depends on the 1D density of the cloud. Inserting this law in Eq. (2) and substituting  $\alpha(z, t) = e^{-\gamma t} \alpha_0(z)$ , we see that  $\alpha_0$  is a solution of

$$\gamma \bar{n}_0(z) \alpha_0(z) + k_B T \partial_z \{G[\bar{n}_0(z)] \partial_z \alpha_0(z)\} = 0. \quad (3)$$

The exponential coefficient  $\gamma$  defines the decay time close to equilibrium and thus the spin drag. This equation can be derived more rigorously from a systematic expansion of Boltzmann's equation (see the Supplemental Material [21]) and is equivalent to the Smoluchowski equation derived in Ref. [17] if one takes for the spin diffusion coefficient  $D = k_B T G / \bar{n}$ . Equation (3) is supplemented by the condition  $\Phi_s(\pm\infty) = 0$  imposed by particle number conservation. Since, as we will show below, the spin conductance is a (nonzero) constant in the dilute limit, this constraint yields the boundary condition  $\partial_z \alpha_0 = 0$  at  $z = \pm\infty$ .

Before solving this equation to find  $\gamma$ , we need to know the expression of the spin conductance  $G$ . We first consider the simpler case of a uniform gas of density  $n_+ = n_- = n_0 = \text{const}$ . Using the method of moments [18], the velocity is a solution of the equation  $\partial_t v_s + \Gamma(n_0) v_s = F_s/m$ , where the spin damping rate  $\Gamma$  is given by

$$\Gamma(n_0) = \frac{1}{n_0} \int d^3\mathbf{p} f_0^{(H)}(\mathbf{p}) p_z C[p_z], \quad (4)$$

where  $f_0^{(H)}(\mathbf{p}) = n_0 e^{-p^2/2mk_B T} / (2\pi mk_B T)^{3/2}$  is the Gaussian phase-space density of a homogeneous gas and  $C[\alpha]$  is the linearized collisional operator defined by

$$C[\alpha](\mathbf{p}_1) = \int d^3\mathbf{p}_2 f_0^{(H)}(\mathbf{p}_2) v_{\text{rel}} \sigma(v_{\text{rel}}) (\alpha_2 - \alpha_1), \quad (5)$$

where  $v_{\text{rel}} = |\mathbf{p}_2 - \mathbf{p}_1|/m$ ,  $\sigma$  is the  $s$ -wave scattering cross section, and  $\alpha_i$  stands for  $\alpha(\mathbf{p}_i)$  [22]. Generally speaking,  $\Gamma$  is proportional to the collision rate, with a numerical prefactor depending on the actual form of the scattering cross section. In the homogeneous case, the stationary velocity is simply given by  $v_s = F_s/m\Gamma(n_0)$ . In a trap, the density profile is inhomogeneous, which leads to a shear of the velocity field and a competition between viscosity and spin drag. Let  $R_{\text{th}} = \sqrt{k_B T/m\omega_{\perp}^2}$  be the transverse size of the cloud and  $\nu$  its kinematic viscosity. Viscosity can be neglected as long as the viscous damping rate  $\nu/R_{\text{th}}^2$  is smaller than  $\Gamma(n_0)$ . Since viscosity scales like  $v_{\text{th}}^2/\gamma_{\text{coll}}$ , with the thermal velocity  $v_{\text{th}} = \sqrt{k_B T/m}$ , this condition is fulfilled as long as  $\Gamma \propto \gamma_{\text{coll}} \gg \omega_{\perp}$ , in other words, when the cloud is hydrodynamic in the transverse direction. In this regime, we can therefore neglect viscous stress and the local velocity  $\mathbf{v}_s(\mathbf{p}) = \int d^3\mathbf{p}' f_s(\mathbf{p}, \mathbf{p}') v_z / n_s(\mathbf{p})$  is simply given by  $\mathbf{v}_s(\mathbf{p}) = F_s/m\Gamma[n_0(\mathbf{p})]$ , where  $n_0(\mathbf{p}) = n_0(0) \exp(-\rho^2/2R_{\text{th}}^2)$  is the local equilibrium density of the cloud.

This scaling for the velocity field is, however, too simple. Indeed, we have  $\Phi_s = \int d^2\mathbf{p} n_0(\mathbf{p}) v_s(\mathbf{p}) \propto \int d^2\mathbf{p} n_0(\mathbf{p}) / \Gamma[n_0(\mathbf{p})]$ , and since  $\Gamma \propto n_0$ , the integral is divergent. This pathology is cured by noting that the hydrodynamic assumption is not valid in the wings of the distribution where the density, and therefore the collision rate, vanish. The breakdown of the hydrodynamic approximation occurs when  $\Gamma[n_0(\rho)] \lesssim \omega_{\perp}$ , i.e., when  $\rho \gtrsim \rho_{\text{max}} = R_{\text{th}} \sqrt{2 \ln(\Gamma_0/\omega_{\perp})}$ , with  $\Gamma_0 = \Gamma[n_0(0)]$  the local spin damping at the trap center. Considering  $\rho_{\text{max}}$  as a cutoff in the integral for  $G$ , we see that  $G \simeq 2\pi \rho_{\text{max}}^2 n_0(0) / m\Gamma_0 \propto \ln(\Gamma_0)/\Gamma_0$ .

In the opposite regime, when the gas is collisionless in the transverse direction, we expect viscous effects to flatten the velocity profile. Assuming a perfectly flat velocity field, then  $v_s \propto F_s/m\Gamma_0$ , and thus  $G = \Phi_s/F_s \propto \bar{n}_0/m\Gamma_0$ .

To make this scaling argument more quantitative, we calculate  $G$  for different physical situations. First, we calculate it numerically using the Boltzmann equation simulation described in Refs. [23,24]. We initialize the axially homogeneous system at thermal equilibrium and then switch on the constant pulling force at  $t = 0$ . In a few collision times, the total spin current of the cloud defined by  $\Phi_s(t) = \langle v_z \rangle_s = \int d^3\mathbf{r} d^3\mathbf{p} f_s(\mathbf{r}, \mathbf{p}, t) v_z$  converges to a constant asymptotic value from which we extract the spin

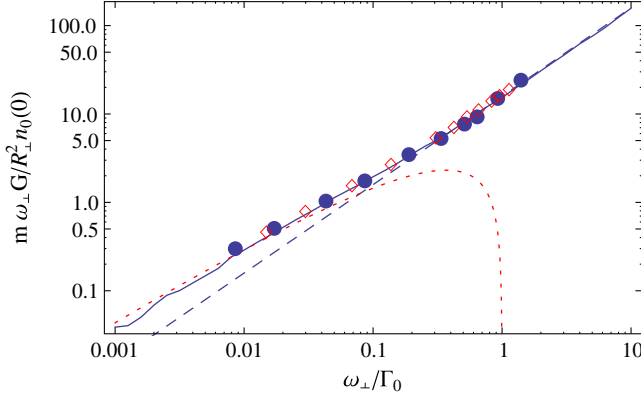


FIG. 1 (color online). Spin conductance  $G$  versus  $\omega_{\perp}/\Gamma_0$ . The dashed blue line represents the collisionless limit  $G \approx 15.87n_0/\Gamma_0$  for a Maxwellian gas. The dotted red line represents the hydrodynamic prediction  $G \approx (2\pi n_0/\Gamma_0) \ln \Gamma_0$ . The solid line represents the semianalytical prediction for the Maxwellian gas (see the Supplemental Material [21]). Molecular dynamics simulation for a constant cross section (blue dots) and a momentum-dependent cross section (open red diamonds) with  $k_{\text{th}}a = 2$ , where  $k_{\text{th}} = \sqrt{mk_B T/\hbar^2}$  is the thermal wave vector.

conductance  $G(\bar{n}_0)$ . Figure 1 shows our results for the spin conductance for a constant cross section  $\sigma = 4\pi a^2$  and a momentum-dependent cross section  $\sigma = 4\pi a^2/(1 + p_{\text{rel}}^2 a^2/4)$  near the unitary limit [25]. When  $G/n_0(0)$  is plotted versus  $\Gamma_0 = \Gamma[n_0(0)]$ , the data points overlap, showing that the drag coefficient depends only weakly on the actual momentum dependence of the scattering cross section. To interpolate between the constant and the unitary cross section, we also study the Maxwellian cross section  $\sigma \propto 1/p$  for which we could find a semianalytical expression of the spin conductance (see the Supplemental Material [21]).

Using these approaches, we find that in the (transverse) collisionless limit  $\Gamma_0 \ll \omega_{\perp}$ , the spin-drag coefficient scales like  $G \approx kn_0(0)R_{\text{th}}^2/m\Gamma_0$ , where  $k \approx 16$  is a numerical coefficient, the value of which depends on the momentum dependence of the scattering cross section (see Table I). For a Maxwellian gas, we find  $k = 15.87$  (see the Supplemental Material [21]). For more general cases, a variational lower bound based on the exact Maxwellian solution yields an estimate very close to the numerical result obtained from the molecular dynamics simulation.

TABLE I. Values of  $k$  for a scattering cross section  $\sigma(p) \propto p^n$  for a constant cross section ( $n = 0$ ), a Maxwellian gas ( $n = -1$ ), and a unitary gas ( $n = -2$ ). For the Maxwellian gas, the lower bound is actually the exact result.

| $n$                     | 0    | -1    | -2   |
|-------------------------|------|-------|------|
| Variational lower bound | 14.5 | 15.87 | 17   |
| Molecular dynamics      | 15.4 | ...   | 18.9 |

In the opposite (hydrodynamic) limit  $\Gamma_0 \rightarrow \infty$ , we recover the expected behavior  $G \approx 2\pi n_0(0)R_{\text{th}}^2 \ln(\Gamma_0/\omega_{\perp})/m\Gamma_0$ .

We also calculate the transverse velocity profile  $v_s(\rho)$  and confirm that it obeys the expected behavior; see Fig. 2. For  $\Gamma_0/\omega_{\perp} \gg 1$ , we recover the viscousless prediction  $v_s \propto 1/\Gamma[n_0(\rho)]$ , while for  $\Gamma_0 \lesssim \omega_{\perp}$ , we obtain a flatter velocity profile as a result of the transverse shearing. We see that in both regimes, the velocity profile is not flat, and this explains the discrepancy between experiment and previous theoretical models based on uniform velocities.

Let us now return to the case of a three-dimensional trap and to the determination of the spin damping rate  $\gamma$ . According to Eq. (3),  $\gamma$  appears as an eigenvalue of the operator  $\hat{S} = k_B T \bar{n}_0^{-1} \partial_z [G(z) \partial_z]$ . This operator is Hermitian on the Hilbert space of functions having a finite limit and zero derivative at  $z = \pm\infty$ , and since at long times the decay is dominated by the slowest mode, we focus on its smallest eigenvalue. We first consider the collisionless limit. In this regime,  $G \propto n_0/\Gamma_0$  is position independent and can be considered as a constant. Using the shooting method [26], we then obtain

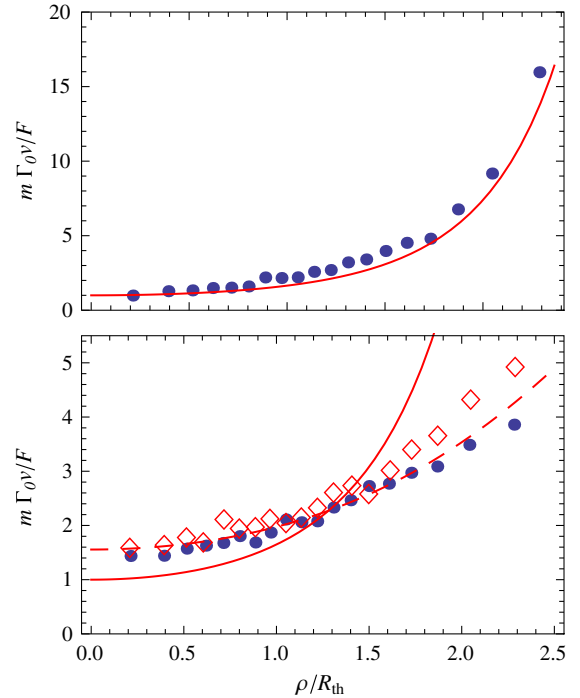


FIG. 2 (color online). Transverse velocity field  $v_s(\rho)$  in units of  $m\Gamma_0/F$  in the infinitely elongated trap. Top: Hydrodynamic regime  $\Gamma_0/\omega_{\perp} \approx 100$ . Bottom: Collisionless regime  $\Gamma_0/\omega_{\perp} \approx 2$ . The blue dots are simulation results for the constant scattering cross section, and the solid red line is the prediction  $v_s(\rho) = F_s/m\Gamma[n_0(\rho)]$  of the hydrodynamic regime. On the lower graph, the empty red diamonds are simulation results for the momentum-dependent cross section at  $k_{\text{th}}a = 2$ , and the dashed red line represents the velocity field of a Maxwellian gas in the collisionless limit (see the Supplemental Material [21]).

$$\gamma \approx 1.342 \frac{k\omega_z^2}{2\pi\Gamma_0}, \quad (6)$$

where the value of  $k$  is given in Table I. For arbitrary values of  $\Gamma_0/\omega_\perp$ , we solve Eq. (3) using for  $G$  a Padé interpolation of the simulation results presented in Fig. 1 (see the Supplemental Material [21]). Following Ref. [15], we take  $\Gamma_{\text{SD}} = \omega_z^2/\gamma$ , and in Fig. 3(a), we plot  $\Gamma_{\text{SD}}/\omega_\perp$  versus  $\Gamma_0/\omega_\perp$ . We compare our model to the experimental results of Ref. [15] and to a direct molecular dynamics simulation of the Boltzmann equation [23]. In this simulation, the atoms are prepared in a harmonic trap of axial frequency  $\omega_\perp = 8\omega_z$ . We displace their centers of mass by a distance  $\pm z_0$ , where  $z_0$  is much smaller than the axial size of the cloud, and we fit the relative displacement versus time to an exponential from which we extract  $\Gamma_{\text{SD}}$ . The results of these simulations are displayed in Fig. 3(a), where they are compared to the solutions of Eq. (3). We observe that the two approaches coincide both for the constant and momentum-dependent cross sections [27].

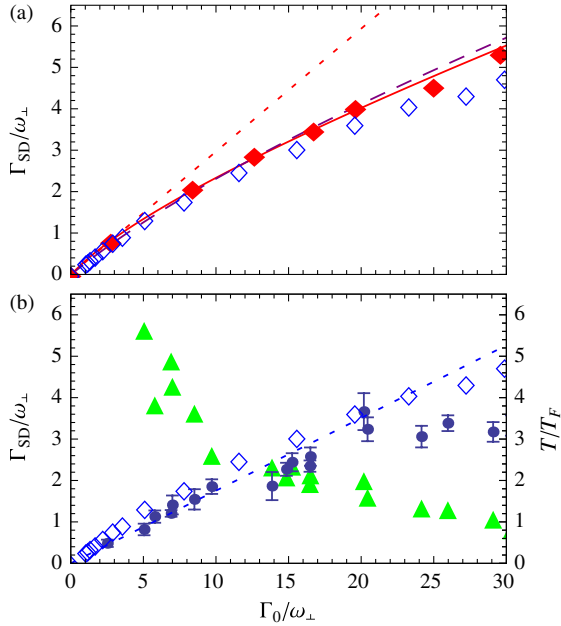


FIG. 3 (color online). Spin-drag coefficient  $\Gamma_{\text{SD}}$  in a harmonic trap. (a): Theoretical predictions. For a constant cross section, the solid red diamonds are the results of the molecular dynamics simulation and the solid red line is the numerical resolution of the eigenequation (3). For a momentum-dependent cross section close to the unitary limit ( $k_{\text{th}}a = 2$ ), the open blue diamonds correspond to the simulation while the dashed blue line is the solution of Eq. (3). The dotted red line is the collisionless prediction  $\Gamma_{\text{SD}} = \Gamma_0/4.03$  for a unitary gas. (b): Comparison with the experimental results of Ref. [15] at unitarity (blue dots). The green triangles represent the associated values of  $T/T_F$ . As above, the open blue diamonds correspond to the simulation at  $k_{\text{th}}a = 2$ . The dotted blue line represents the experimental fit  $\Gamma_{\text{SD}} \approx \Gamma_0/5.7$ . For the experimental data,  $\Gamma_0$  is calculated using the theoretical value Eq. (4) for the unitary gas.

As observed in Fig. 3(b), theory and experiment agree remarkably as long as  $T/T_F \gtrsim 2$ . Beyond that limit, we enter the quantum degenerate regime where the Boltzmann equation is no longer valid, and, as expected, we observe that experiment and theory deviate from each other. In the high-temperature, collisionless limit, we find for the “unitary” value  $k = 18.9$ ,  $\Gamma_{\text{SD}} \approx \Gamma_0/4.03$ . This result differs from the high-temperature value  $\Gamma_{\text{SD}} \approx \Gamma_0/5.7$  found in Ref. [15]. We interpret this discrepancy by noting that the theoretical asymptotic behavior Eq. (6) is valid for  $\Gamma_0/\omega_\perp \lesssim 5$ , while the experimental value was obtained by linear fitting the points with  $\Gamma_0/\omega_\perp \lesssim 15$ , i.e., in a regime where the gas was likely less collisionless. Fitting our data on the same scale using a linear law would indeed give  $\Gamma_{\text{SD}} \approx \Gamma_0/5.0$ . We also note that our scaling  $\Gamma_{\text{SD}} = \omega_\perp f(\Gamma_0/\omega_\perp)$  contradicts the scaling  $\hbar\Gamma_{\text{SD}} = E_F g(T/T_F)$ , where  $E_F = k_B T_F$ , used in Ref. [15] to analyze the experimental data. The two scalings agree only in the collisionless limit where  $f$  is linear, hence outside of the region explored by experiments.

In summary, we have studied the classical dynamics of spin transport in a trap using the Boltzmann equation approach. By taking into account *ab initio* the trap inhomogeneity, we are able to reproduce the experimental results without uncontrolled approximations and obtain several robust results which allow for a more rigorous extraction of transport coefficients from measurements in trapped cold gases. We highlight the competition between viscosity and spin drag in the shape of the velocity profile which is a crucial ingredient in the understanding of transport properties in a trap. We also demonstrate the breakdown of the universal scaling used to interpret the data of Ref. [15] in the experimentally relevant range of parameters. In the future, we anticipate extending this approach to lower temperatures where many-body interactions and Pauli blocking play a significant role. In this regime, strong correlation effects are taken into account by a renormalization of the Landau parameters of the system [20].

We thank M. Zwierlein and A. Sommer for fruitful discussions and for providing us with the experimental data of Fig. 3. O.G. acknowledges support from the Excellence Cluster “Nanosystems Initiative Munich (NIM).” F.C. acknowledges support from ERC (Advanced Grant Ferlodim and Starting Grant Thermodynamix), Région Ile de France (IFRAF), and Institut Universitaire de France. C.L. acknowledges support from EPSRC through Grant No. EP/I018514.

- [1] *The BCS-BEC Crossover and the Unitary Fermi Gas*, edited by W. Zwerger, Lecture Notes in Physics Vol. 836 (Springer, Berlin, 2012).
- [2] J.-P. Brantut, J. Meineke, D. Stadler, S. Krinner, and T. Esslinger, *Science* **337**, 1069 (2012).

- [3] C. Cao, E. Elliott, J. Joseph, H. Wu, J. Petricka, T. Schäfer, and J. E. Thomas, *Science* **331**, 58 (2011).
- [4] P. K. Kovtun, D. T. Son, and A. O. Starinets, *Phys. Rev. Lett.* **94**, 111601 (2005).
- [5] Y. A. Liao, M. Reville, T. Paprotta, A. S. C. Rittner, W. Li, G. B. Partridge, and R. G. Hulet, *Phys. Rev. Lett.* **107**, 145305 (2011).
- [6] G. M. Bruun, *Phys. Rev. A* **85**, 013636 (2012).
- [7] T. Enss and R. Haussmann, *Phys. Rev. Lett.* **109**, 195303 (2012).
- [8] C. H. Wong, H. T. C. Stoof, and R. A. Duine, *Phys. Rev. A* **85**, 063613 (2012).
- [9] H. Heiselberg, *Phys. Rev. Lett.* **108**, 245303 (2012).
- [10] R. Kittinaradorn, R. Duine, and H. Stoof, *New J. Phys.* **14**, 055007 (2012).
- [11] H. Kim and D. A. Huse, *Phys. Rev. A* **86**, 053607 (2012).
- [12] K. MUSAELIAN and A. MEYEROVICH, *J. Low Temp. Phys.* **89**, 535 (1992).
- [13] V. P. Mineev, *Phys. Rev. B* **69**, 144429 (2004).
- [14] S. Wolf, D. Awschalom, R. Buhrman, J. Daughton, S. Von Molnar, M. Roukes, A. Y. Chtchelkanova, and D. Treger, *Science* **294**, 1488 (2001).
- [15] A. Sommer, M. Ku, G. Roati, and M. W. Zwierlein, *Nature (London)* **472**, 201 (2011).
- [16] A. Sommer, M. Ku, and M. W. Zwierlein, *New J. Phys.* **13**, 055009 (2011).
- [17] G. M. Bruun and C. J. Pethick, *Phys. Rev. Lett.* **107**, 255302 (2011).
- [18] L. Vichi and S. Stringari, *Phys. Rev. A* **60**, 4734 (1999).
- [19] S. Chiacchiera, T. Macri, and A. Trombettoni, *Phys. Rev. A* **81**, 033624 (2010).
- [20] G. M. Bruun, *New J. Phys.* **13**, 035005 (2011).
- [21] See Supplemental Material at <http://link.aps.org/supplemental/10.1103/PhysRevLett.111.190402> for details on the calculation of the spin drag of the Maxwellian gas, as well as on the Padé interpolation of the spin conductance.
- [22] Strictly speaking, the expression for  $\Gamma$  in Eq. (4) was obtained using an uncontrolled ansatz for the phase-space density. Using a molecular dynamics simulation, we checked that this ansatz does indeed yield very accurate results for the homogeneous gas.
- [23] O. Goulko, F. Chevy, and C. Lobo, *Phys. Rev. A* **84**, 051605 (2011).
- [24] O. Goulko, F. Chevy, and C. Lobo, *New J. Phys.* **14**, 073036 (2012).
- [25] For practical reasons, we limited our study of the strongly interacting regime to  $k_{\text{th}}a = 2$ . For this value, the difference with the unitary gas prediction for the value of  $\Gamma$  is only 10%.
- [26] W. H. Press, S. A. Teukolsky, W. T. Vetterling, and B. P. Flannery, *Numerical Recipes: The Art of Scientific Computing* (Cambridge University Press, Cambridge, England, 2007), 3rd ed..
- [27] In the case of the momentum-dependent cross section, we observe a  $\approx 10\%$  deviation at a large collision rate that we interpret as resulting from a systematic error of the same order of magnitude introduced by the Padé approximation of the spin conductance.